

# Dry and Wet Periods in Eastern China Watersheds: Patterns and Predictability\*

Isabella BORDI<sup>1</sup>, Klaus FRAEDRICH<sup>2</sup>,  
JIANG Jianmin<sup>3</sup> & Alfonso SUTERA<sup>1</sup>

(1: Department of Physics, University of Rome "La Sapienza", Rome Italy; 2: Institute for Meteorology, University of Hamburg, Hamburg Germany; 3: Training Centre of China Meteorological Administration, Beijing 100081, P.R. China)

**Abstract** Rain gauge observations are the basis for an analysis of the time-space variability of dry and wet periods during the last fifty years in nine Chinese watersheds. The Standardized Precipitation Index (SPI) is introduced to assess the climatic conditions on a biennial time-scale. To capture the spatial pattern of co-variability principal component analysis (PCA) is applied to the watersheds SPI time series. Results suggest that the index low-frequency variability for watersheds is well described by that of three main areas: regions near the Yellow river, regions nearby the Yangtze River and Huaihe or Zhujiang Basin. Furthermore, the analysis shows that the northern basins from the seventies is experiencing dry conditions more frequently, which is due to the presence of a negative trend in the SPI time series. It is perhaps related to long-term periodicities that characterise the SPI signal (say 24 and 48 year). Together with these long periods there are other ones contributing to the power spectrum variance ranging from 3 up to 9 year. These periodic components in the index time series provide good chances for the long-term predictability of dryness and wetness.

**Keywords:** dry and wet period, eastern of china, predictability

Low frequency variability of the climate system manifests itself in fluctuations of the sea surface temperature over some regions of the oceans<sup>[1]</sup> and in drought and wetness variability over the continents<sup>[1-3]</sup>. Before analyzing sea surface temperature fluctuations affecting drought and wetness over the continents, regional case studies are required to test suitable drought/wetness indicators. Formidable test beds are China and Europe at the eastern and western boundaries of the Eurasian continent: China with its exposure to highly complex atmospheric circulation regimes affected by the monsoonal systems and mid-latitude disturbances, Siberia and the Himalayan mountains and Europe at the sensitive tale end of the North Atlantic stormtrack. Thus, it is not surprising that these are regions, which suffer wet or dry spells causing serious water shortage or extreme floods. Such extreme events have been reported for the Yangtze and other watersheds in China, which attracted attention because of the severity and damages. These phenomena initiated our study and co-operation to search for their potential of prediction by analyzing the recent history, identifying possible mechanisms, and evaluating the anticipated skill. Here the

---

\* Received: 2003-08-01; Accepted: 2003-11-23. Isabella BORDI, female, email: bordi@romatm9.phys.uniroma1.it.

emphasis lies on the longer time scales involved. At first glance, the processes are governed by different time scales: the extended dry or wet periods are associated with long-term variability, whereas floods are triggered by the short term and intensive event of a single or a fast sequence of frontal or convective complexes. However, when the long-term behavior is considered, the two climate extremes may be a realization of a common underlying mechanism.

Here we extend and complement studies on eastern China dryness and wetness<sup>[4-6]</sup>, which describe low frequency variability and abrupt changes during the last five hundred and thousand years exploiting qualitative historical data. The last fifty years of instrumental precipitation records for nine watersheds are analyzed using the Standardized Precipitation Index<sup>[3,7-10]</sup>. The SPI characterizes the water deficit and surplus by the precipitation field alone. It can be easily computed, and, as the index is standardized, it is also suitable for comparing different regions<sup>[11]</sup>. Thus, the SPI is a useful tool to be established operationally as part of a drought watch system to monitor dryness and wetness. The paper is organized as follows. Section 2 describes the data analyzed and the methods applied; section 3 analyses the space-time variability of the watersheds. An outlook on Yangtze basin (internal variability and potential predictability of dryness and wetness) follows in section 4, while conclusions are in section 5.

## 1 Data and methods of analysis

Periods of wetness and dryness are characterized by an index, which depends only on the monthly mean precipitation recorded at single stations. The 160 stations in China, from 1951 to 2000, are chosen because of their record length and the lack of missing values (see Fig. 1a for their location). The analysis is focussed on the monthly mean precipitation time series of nine watersheds in central-eastern China (based on 16, 10, 7, 28, 7, 45, 5, 4, 14 stations, respectively). The river basins are numbered from north to south: (1) Heilongjiang, (2) Liaohe, (3) Haihe, (4) Huanghe (Yellow River), (5) Huaihe, (6) Yangtze River, (7) Qiantangjiang, (8) Minjiang, and (9) Zhujiang Rivers. The location of the nine main river basins is shown in Fig. 1b. All time series are subjected to the following analysis.

**Standardized Precipitation Index (SPI):** The SPI is defined to describe periods of dryness and wetness. It is based on time series of monthly precipitation cumulated over a given period (time scale ranging from weeks to years). It assumes that the empirical distribution of precipitation frequency for the selected time scale and for a given month of the year follows a Gamma probability density function. Then an equal probability transformation from a Gamma to a Normal distribution is applied. Thus, the SPI is the number of standard deviations that precipitation deviates from the mean<sup>[8-9]</sup>. The mapping into a normal distribution allows assessing dry and wet periods at the same strength, and, most importantly, enables to compare climatic conditions occurring in different areas with different hydrological regimes. Since the SPI is computed for finite time scales, the various kinds of droughts, such as meteorological, agricultural or hydrological, occurring on multiple time scales, may be monitored<sup>[11]</sup>. A window length of 24 months has been proven as a suitable time scale (SPI-24), which captures the low frequency variability

avoiding an explicit annual cycle. Note that short-time windows are not the focus of this analysis as we are primarily interested to the long-term aspect of dryness and wetness. According to the classification of the index values a level crossing at  $SPI = +/-2$  indicates transition to extreme wetness/dryness<sup>[3]</sup>.

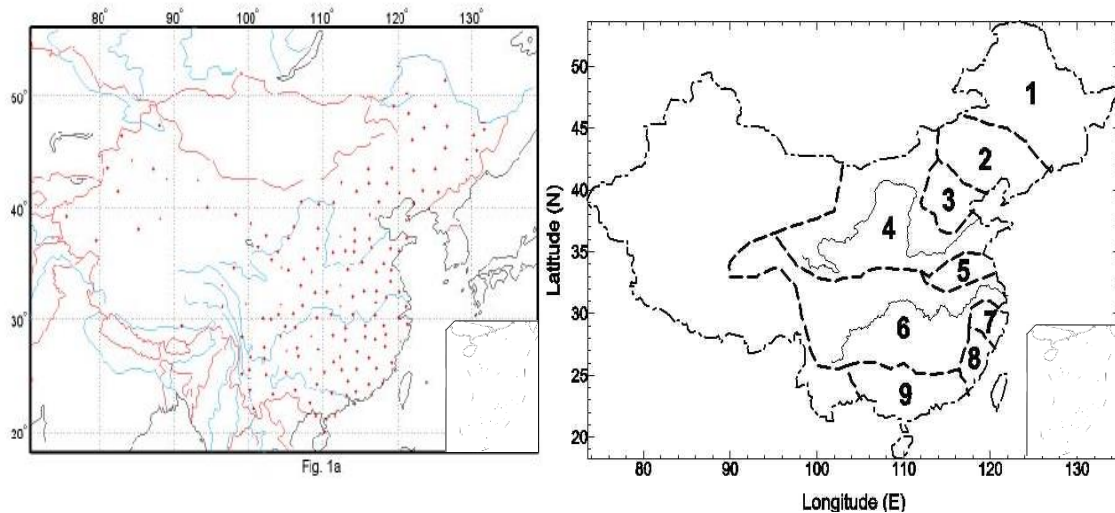


Fig.1 Location of stations (160) in China (a) and the nine watersheds (b) in Central-Eastern China

**Principal component analysis and power spectra:** The patterns of covariability of SPI for different stations are determined by principal component analysis (PCA), which reduces the data to generate a set of linearly independent spatial patterns (loadings). They display spatial variability by spatial modes or patterns, which describe the statistical correlation between the SPI-series and the corresponding score (principal component or PC time series). These patterns are ordered with respect to their contribution to the total space-time variability (in percent; see<sup>[3,12]</sup>). Moreover, it may be useful to rotate the loadings in a way that the resulting ones are more spatially localised, i.e. the rotated loadings have high correlation with a smaller set of spatial variables and little correlation with the remained variables. In the present study this technique will allow to find areas within the region that have rather independent climatic variability. Here, only orthogonal rotations are considered and they are computed according to the VARIMAX criterion<sup>[12]</sup>. Of course, each rotated pattern will not explain the same variance as the unrotated one, although the total variance explained remains unchanged. To identify time variability, the scores (PCs) are subjected to power spectrum analysis to identify their behaviour in the frequency domain<sup>[13]</sup>: Spectral peaks and gaps characterise distinct periodicities while power-law scaling in a sufficiently wide frequency band may indicate long-term memory effects.

## 2 Eastern China watersheds: space-time variability

By applying the PCA to the SPI-24 computed for the nine watersheds we obtain the following results:

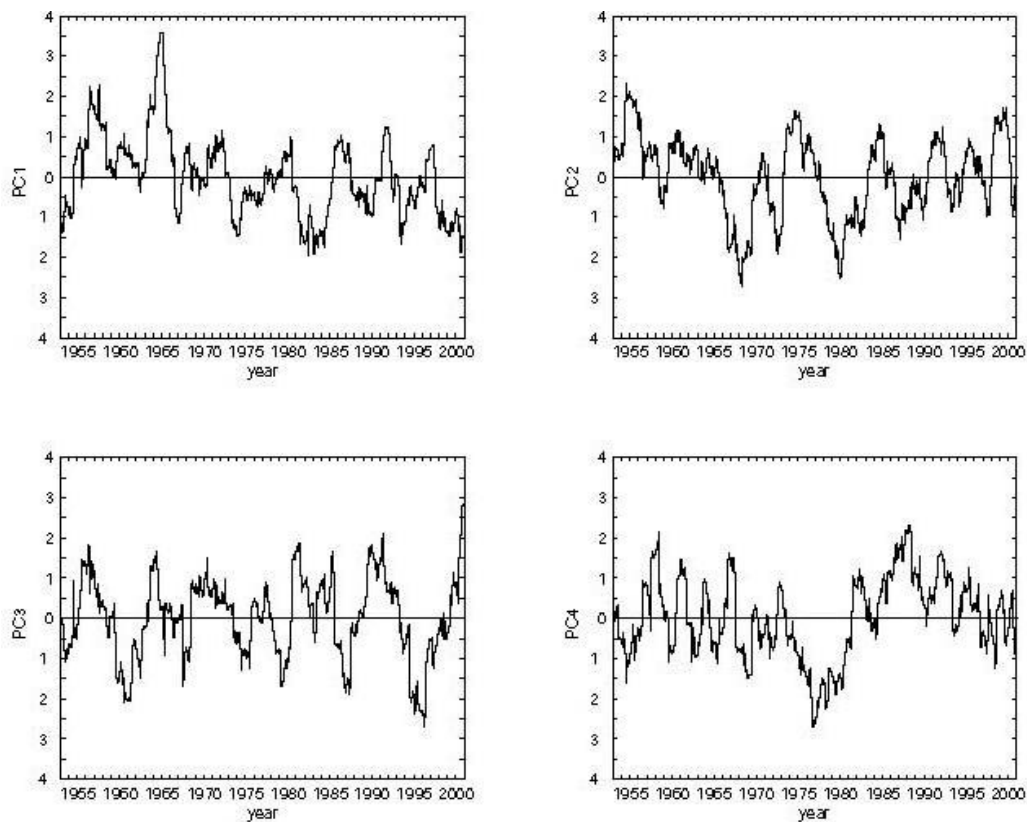


Fig.2 Time series of the first four principal component scores (PC) of the SPI-24 for watersheds 1-9

(1) The first four watershed loadings explain about 80.6% of the total variance (Tab. 1) compared with 35.5% cumulative variance explained by the first four loadings of China stations<sup>[14]</sup>. PC-1 and PC-2 explain about the same amount of variance and the same occurs for PC-3 and PC-4 (we try to solve this problem later on in the analysis). The corresponding PC scores (Fig. 2) vary similar to those obtained for the whole China SPI-24 (not shown) with correlation coefficients of 0.84, 0.87, 0.59, 0.86. Inspection of loading values (Tab. 2) suggests that SPI time series in basins 2-5 are highly correlated with PC-1 (the negative trend characterises these basins, in particular basin 3 and 4), those of basins 6-8 are highly correlated with PC-2, while basin 9 shows high anti-correlation with PC-3. Only SPI time series in basin 1 is highly correlated with PC-4. The PC-4 time series shows a “singular” behaviour raising some doubt on the quality of precipitation time series. Furthermore, the fourth loading suggests that the feature that characterises basins 1 is not in common with any other basin. Thus, we decide to omit basin 1 from the analysis. (ii) Omitting basin 1, which is sufficiently well represented by PC-4, the cumulative variance explained by the first three loadings (Tab. 3) is, as expected, reduced to about 76%. On the other hand, the variances explained by loadings are higher and, more importantly, they are not so close to one another compared to the previous case. The loading values and the corresponding PC scores are shown in Tab. 4 and Fig. 3 respectively. Loading values suggest that the

watersheds 2-5 (6-9) are in phase (anti-phase) with the first PC-1. Furthermore, loadings show that basins 2-4 are highly positive correlated with PC-1; basins 6-8 positive correlated with PC-2 and basins 5 and 9 correlate and anti-correlate with PC-3. Employing an orthogonal VARIMAX rotation, the spatial structure is emphasised with higher values in the rotated loadings (see Tab. 5). The associated PC scores (Orths) are shown in Fig. 4. Results confirm those obtained with PCA even if the scores time series are lightly changed. This means that the SPI-24 low-frequency variability of watersheds is well characterised by that of three main areas: basins 2-4 (regions around the Yellow river), 6-8 (regions nearby the Yangtze river) and 5/9 (in fact, basins 5 and 9 are explained by the same score Orth-3). These three areas contribute to about 76% of the total variance of the eight watersheds considered.

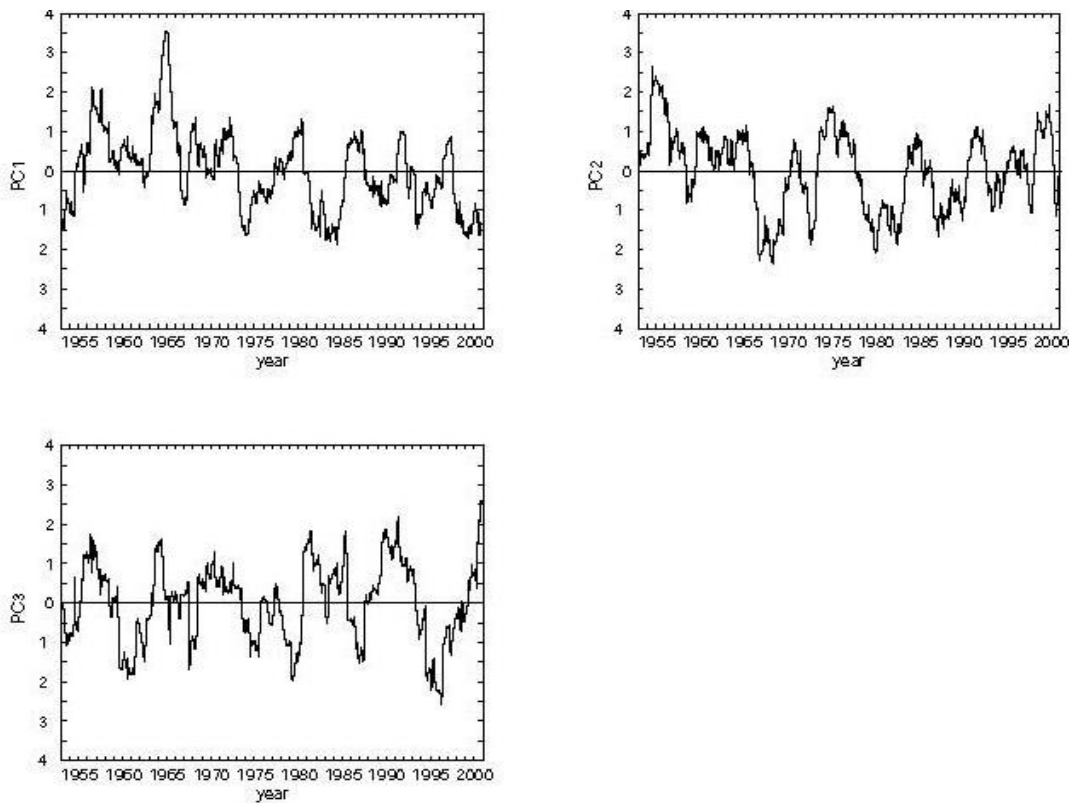


Fig.3 Time series of the first three principal component scores of the SPI-24 for watersheds 2-9

Tab. 1 Percentages of variance explained by the first four loadings of the SPI-24 for watersheds 1-9

n. PCs	% variance for 9 watersheds
1	29.8
2	27.8
3	12.1
4	10.9
Cumulative variance (%)	80.6

Tab. 2 First four loadings of the SPI-24 for watersheds 1-9.the explained variance is shown in Table 1

n. River basins	Loading 1	Loading 2	Loading 3	Loading 4
1	0.181	0.471	-0.174	0.810
2	0.641	0.404	-0.532	0.073
3	0.733	0.378	-0.155	-0.263
4	0.701	0.267	-0.096	-0.398
5	0.520	0.395	0.499	0.127
6	-0.260	0.775	0.369	-0.187
7	-0.462	0.800	0.067	0.014
8	-0.507	0.698	-0.104	-0.142
9	-0.631	0.142	-0.582	-0.156

Tab.3 Percentages of variance explained by the first three loadings of the SPI-24 for watersheds 2-9

n. PCs	% variance for 8 watersheds
1	33.3
2	29.4
3	13.5
Cumulative variance (%)	76.2

Tab.4 First three loadings of the SPI-24 for watersheds 2-9. The explained variance is shown in Table3

n. river basins	Loading 1	Loading 2	Loading 3
2	0.552	0.477	-0.515
3	0.657	0.537	-0.206
4	0.648	0.436	-0.170
5	0.439	0.476	0.509
6	-0.390	0.753	0.322
7	-0.601	0.694	0.063
8	-0.624	0.607	-0.132
9	-0.645	0.030	-0.600

Power spectrum: The power spectra of the first three PC scores of the VARIMAX rotated loadings are documented in Fig. 5. A broad band peak is found in all the three spectra centered around 3.7-4.0 year suggesting a link with the El Niño/Southern Oscillation (ENSO) phenomenon. At 95% confidence level, the power spectrum of Orth-1 has statistical significant peaks at 5.3, 3.7 and 2.8 year, Orth-2 at 3.7 and Orth-3 at 6.9, 4.0 year. Considering the 95% confidence interval on a single spectral line, also other peaks might be statistical significant such as 9.6 year in Orth-1 or 9.6 and 2.4 year in Orth-2. Each spectral band consists of all significant frequencies, which contribute to the statistically significant peaks. It must be pointed out that the trend detected in Orth-1, which seems to be linear, is possibly related to the long periods (say 48 and 24

year, see the raising in the power spectrum approaching zero frequency), although their statistical significance cannot be ascertained due to the short time series available. Periodicities, similar to those unveiled, have also been found in the SPI computation for Europe based on NCEP/NCAR re-analysis data<sup>[3]</sup>. Furthermore, they are surprisingly close to those found for other regions analysed in some detail<sup>[15]</sup> even if they explain different percentages of spectral variance.

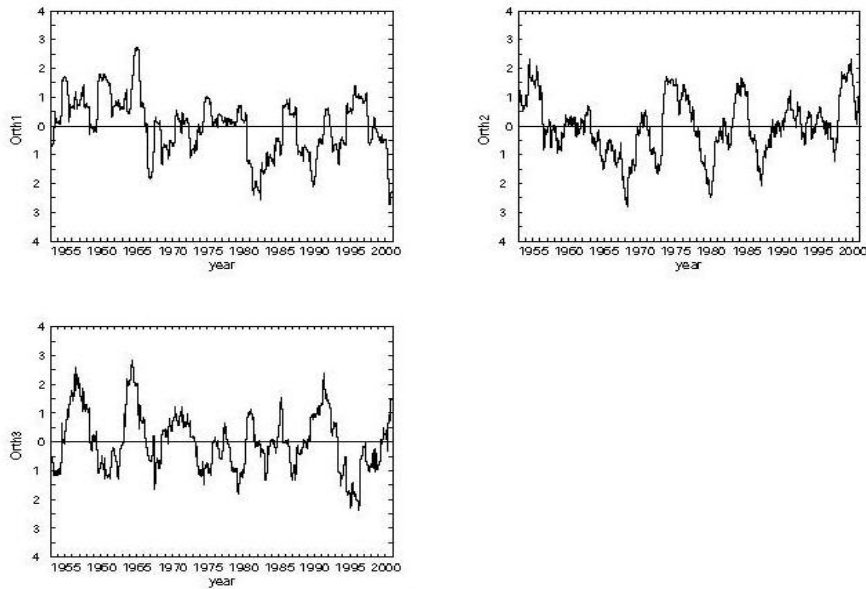


Fig.4 Time series of the three VARIMAX rotated principal component scores (Orth) of the SPI-24 for watersheds 2-9

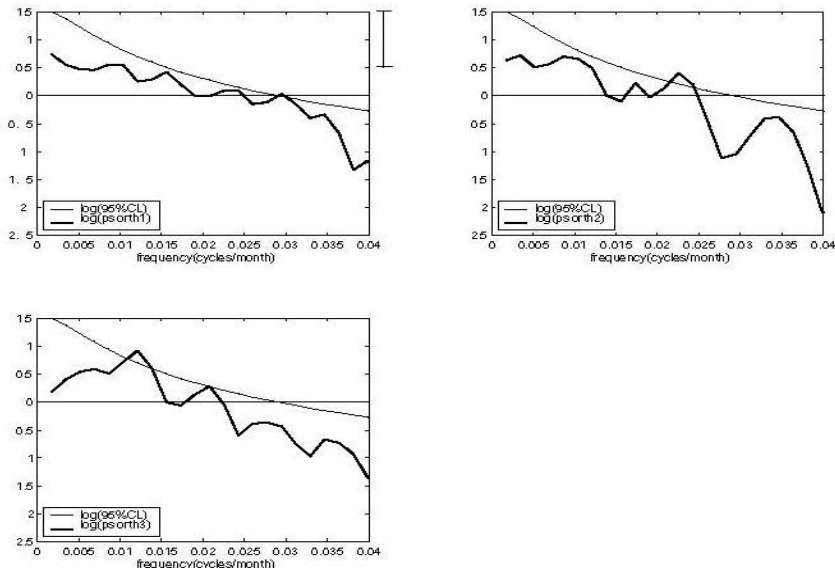


Fig.5 Logarithm of the power spectra (ps) of the three VARIMAX rotated principal component scores for watersheds 2-9. Thin line is the first order autoregressive adapted to the time series (with the same mean and variance, Jenkins and Watts 1968). The vertical line is the 95% confidence interval

### 3 Yangtze watershed: internal variability and potential predictability

Since dryness and wetness seem to be characterised by the periodicities outlined above, a simple method to predict the occurrence of these climatic phenomena is that based on the forward extrapolation of the periodic components present in the signals. As an example we analyse the Yangtze watershed considering the region  $100^{\circ}\text{E} < \text{lon} < 124^{\circ}\text{E}$  and  $26^{\circ}\text{N} < \text{lat} < 33^{\circ}\text{N}$  near the Yangtze River.

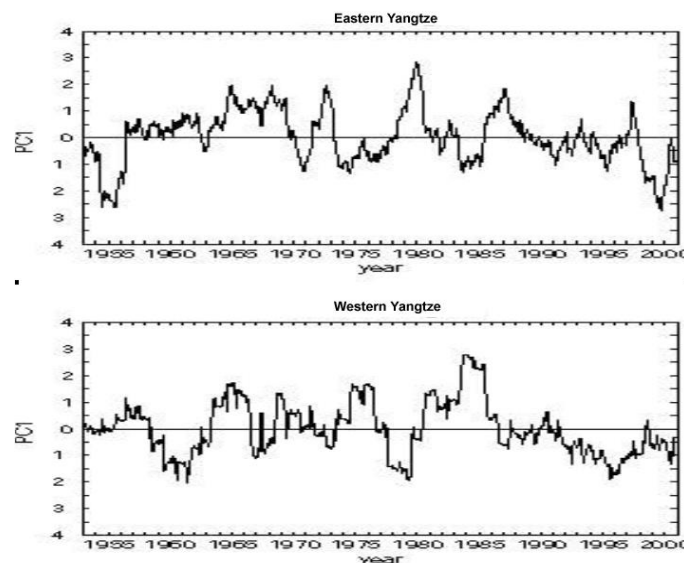


Fig.6 Time series of the first principal component score of the SPI-24 for eastern Yangtze (upper) and western Yangtze (lower) Watershed

Internal variability: There are 28 stations for the eastern part and 20 for the western one (we set the line separating east and west part at  $\text{lon}=110\text{E}$ ). It must be noted that this is merely a qualitative analysis, because we analyse a spatially inhomogeneous station distribution and there is a different number of stations for the two sub-regions. Again, the basis is the principal component analysis, which is applied to the SPI-24 station time series, before single station predictability analysis is performed. The following results are obtained from PCA: (i) The first loading for the eastern Yangtze (see Tab. 6), that explains 38.4% of the total variance, shows anti-correlation in the whole domain with the corresponding score (Fig. 6 upper panel). The first principal component score is close to the PC-1 obtained for eastern China<sup>[14]</sup> (correlation coefficient 0.7), but has also anti-correlation with PC-2 of eastern China (correlation coefficient -0.6). (ii) The first loading for western Yangtze (see Tab. 6) explains 18.8% of the total variance and the corresponding score is shown in Fig. 6 (lower panel). PC-1 is very close to that obtained for PC-2 for eastern China (correlation coefficient 0.6). Thus, the climatic conditions of eastern and western Yangtze are not fully separable. The conclusion is the same if we apply a VARIMAX rotation to the principal components of the whole Yangtze region.



Tab.5 The main three VARIMAX rotated loadings of the SPI-24 for watersheds 2-9

n. river basins	Rotated Loading 1	Rotated Loading 2	Rotated Loading 3
2	.890	-.008	-.065
3	.833	.019	.261
4	.752	-.051	.266
5	.289	.193	.747
6	.001	.873	.245
7	-.035	.915	-.090
8	.002	.833	-.285
9	-.093	.321	-.816

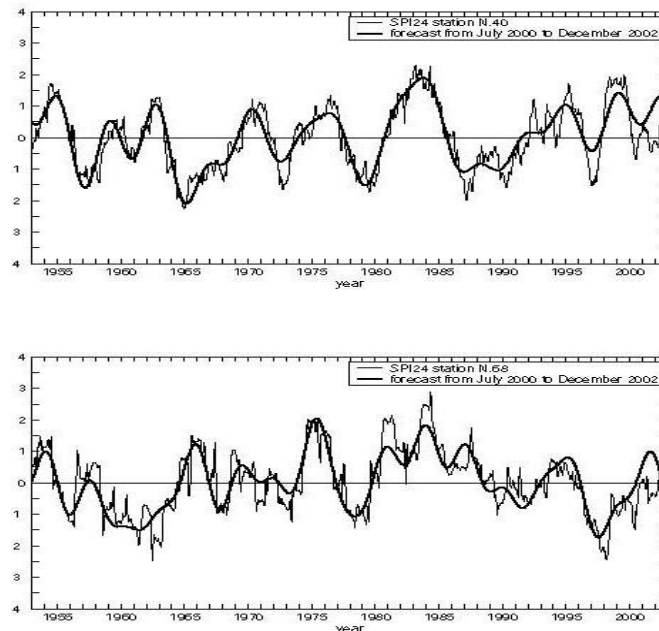


Fig.7 Time series of the SPI-24 from December 1952 to August 2002 (thin line) and the “forecast” from July 2000 to August 2002 (thick line) obtained extrapolating the periodic components of the signal for stations N.40 (eastern Yangtze, upper) and N.68 (western Yangtze, lower)

Potential predictability: We use the results above for selecting sample stations in the two sub-regions that are well anti-correlated/correlated (-0.7/0.7) with the corresponding first loading. They are station N<sub>0</sub>40 = (27.05° N, 114.55° E) in the eastern and station N<sub>0</sub>68 = (31.16° N, 107.28° E) in the western part of the watershed<sup>①</sup>. Power spectra of the SPI-24 at these two stations (not shown) have statistically significant periodicities at roughly the same sequence of frequencies of Orth-2 that characterises basins 6-8. To test the potential predictability of the SPI-24 time series at these two stations, we first select periods that explain at least 2% of the spectral variance

<sup>①</sup> The numbering of stations refer to eastern China data set

(these are band periods contributing to the statistical significant peaks) training the signal till June 2000. Then the periodic component of the index time series is extrapolated forward from July 2000 up to December 2002 and compared with the updated SPI-24 series. The results are summarised in Fig. 7. The method seems to provide a good result, keeping in mind that only a predictability of the envelop of the index is expected, which leaves the high frequencies fluctuations unresolved<sup>[14,16]</sup>.

Tab. 6 First loading of the SPI-24 for eastern Yangtze and western Yangtze. the corresponding PC-1 scores are shown in Fig.6

n. stations	Loading 1 Eastern Yangtze	Loading 1 Western Yangtze
1	-0.204	-0.208
2	-0.160	0.048
3	-0.021	-0.100
4	-0.151	0.267
5	-0.488	0.644
6	-0.438	0.721
7	-0.456	0.409
8	-0.810	0.469
9	-0.704	0.581
10	-0.803	0.696
11	-0.866	0.044
12	-0.628	-0.122
13	-0.437	0.433
14	-0.707	-0.349
15	-0.305	-0.361
16	-0.705	-0.065
17	-0.764	-0.127
18	-0.855	-0.185
19	-0.540	0.712
20	-0.769	0.688
21	-0.275	
22	-0.830	
23	-0.865	
24	-0.645	
25	-0.716	
26	-0.775	
27	-0.506	
28	-0.544	

## 4 Conclusion

The analysis proposed here extends and complements previous studies based on long time series of precipitation data of eastern China<sup>[4-5,16]</sup>, which revealed multidecadal to centennial variations and show that, when a dry condition was observed in southern China, a wet situation was found in the northern part and vice versa. The last fifty years of observed precipitation records for the nine most important watersheds are subjected to the SPI analysis to provide an objective assessment of dryness and wetness on a biennial time-scale. Results suggest that the SPI-24 low-frequency variability of watersheds is well described by that of three main areas: basins 2-4 (regions around the Yellow river), 6-8 (regions nearby the Yangtze river) and 5/9 (in fact basins 5 and 9 are explained by the same score Orth-3). These three areas contribute to about 76% of the total variance of the eight watersheds considered. Furthermore, the PCA of the SPI time series shows that, beginning with the seventies, the northern side of the eastern China (i.e. basins 2-4) is experiencing more frequently drought events due to the presence of a negative trend in the SPI series. This may be probably associated with long-term periodicities, whose statistical significance cannot be ascertained, because of the short time series available. Other periods contribute to the power spectrum variance spanning from 3 to 9 year. It should be mentioned that similar frequencies occur in Europe employing SPI analysis to NCEP/NCAR data and rain gauge observations in the Sicily-Elbe regions.

An analysis focused on the regions nearby the Yangtze River, suggests that the long-term variability of eastern and western Yangtze, even if there are differences between the two sub-regions, is not fully separable. We use this result to select two stations, characteristic of the eastern and western sub-regions, for testing the potential predictability of dryness and wetness extrapolating forward the periodic components present in the stations SPI series. Results provide good changes for long-term “forecast” and useful resources for the design of a more rigorous statistical forecast model for dry and wet occurrences.

Acknowledgements: Bordi and Sutera acknowledge the financial supports provided by CNR (grant Accordo di Programma MURST-CNR Ecosistemi Marini ) and ASI (grants CLOUDS, GEO-MED, CASSINI and GOMAS).

### References

- 1 Fraedrich K, R Blender. Scaling of atmosphere and ocean temperature correlations in observations and climate models. *Phys Rev Lett*, 2003, 90: 108501(1-4)
- 2 Svoboda M D, LeComte M, Hayes R, et al. The Drought Monitor. *Bull Amer Meteor Soc*, 2002, 83: 1181- 1190
- 3 Bordi I, A Sutera. Fifty years of precipitation: some spatially remote teleconnections. *Water Res Manage*, 2001,15: 247-280
- 4 Wang S W, Zhao Z C. Droughts and floods in China, 1470-1979. In: T M L. Wigley M J. Ingrasham et al. Eds, *Climate and History*, Cambridge University Press, 1981:171-288
- 5 Clegg S L, Wigley T M L. Periodicities in precipitation in north-east China, 1470-1979. *Geophys Res Lett*, 1984, 11: 1219-1222

- 6 Jiang J, Zang D, Fraedrich K. Historic climate variability of wetness in East China (1960-1992): A wavelet analysis. *Intern J Climatology*, 1997, 17: 969-981
- 7 McKee T B, Doesken N J, Kleist J. The relationship of drought frequency and duration to time scales. Preprints, 8<sup>th</sup> Conference on Applied Climatology, 17-22 January, Anaheim, CA. *Amer Meteor Soc*, 1993:179-184
- 8 Guttman N B. Accepting the Standardized Precipitation Index: a calculation algorithm. *J Amer Water Resour Assoc*, 1999, 35: 311-322
- 9 Keyantash J, Dracup J A. The quantification of drought: an evaluation of drought indices. *Amer Meteor Soc*, 2002, 83: 1167-1180
- 10 Bordi I, Sutera A. An analysis of drought in Italy in the last fifty years. II *Nuovo Cimento*, 2002,25C: 185-206
- 11 Hayes M J, Svoboda M D, Wilhite D A, et al. Monitoring the 1996 drought using the standardized precipitation index. *Bull Am Meteor Soc*, 1999, 80: 429-438
- 12 Rencher A C. Multivariate statistical inference and applications. New York: John Wiley Sons, 1998: 559
- 13 Jenkins G M, Watts D G. Spectral analysis and its applications. Holden-Day, Inc, 500 Sansome Street, San Francisco, California, 1968. 525
- 14 Bordi I K, Fraedrich F W, Jiang J, et al. Fluctuations and patterns of dry and wet periods: Eastern China. *Theor Climatol*, 2003: Submitted
- 15 Qi H, Feng S. A southward migration of centennial-scale variations of drought/flood in eastern China and the western United States. *J Climate*, 2001, 14: 1323-1328
- 16 Bordi I K, Fraedrich F W, Gerstengarbe P C, et al. Potential predictability of dry and wet periods: Sicily and Elbe-Basin (Germany). *Theor Climatol*, 2003: Submitted

## 中国东部诸流域的干旱和湿润期：模式和预测

Isabella BORDI<sup>1</sup>, Klaus FRAEDRICH<sup>2</sup>, 江剑民<sup>3</sup> & Alfonso SUTERA<sup>1</sup>

(1: Department of Physics, University of Rome "La Sapienza", Rome Italy; 2: Institute for Meteorology, University of Hamburg,

Hamburg Germany; 3: 中国气象局培训中心, 北京 100081)

### 摘要

降水观测记录是近 50a 来中国九大流域干旱和湿润期时空变化分析的基础. 以两年为时间尺度引入标准降水指数 (SPI) 来分析评价气候变化情景, 结果表明黄河流域、长江流域和淮河 (或珠江) 流域等三个主要的区域表现为低频率变化指数: 另外分析显示北方地区自 20 世纪 70 年代以来干旱更频繁的出现, 在 SPI 时间序列中呈现负趋势变化. 这也许与表征 SPI 信号的长周期有关 (24a 和 48a 周期). 与这些长周期一起, 也有一些其它方面的因素有助于频谱变化, 范围从 3a 到 9a 不等. 在指数时间序列中这些周期成分的存在为长期预测干旱和湿润期提供了很好的条件.

**关键词** 干旱和湿润期 中国东部 预测

**分类号** P426. 61<sup>4</sup>